



Design and Analysis of a Combined Savonius-Darrieus Wind Turbine for Irrigation Application

Mahdi Shahmari, Payam Zarafshan*, Shahriar Kouravand, Morteza Khashehchi

Department of Agro-Technology, College of Aburaihan, University of Tehran, Pakdasht, Tehran, Iran.

PAPER INFO

Paper history:

Received 18 March 2020

Accepted in revised form 21 July 2020

Keywords:

Irrigation
Combined Savonius-Darrieus Wind Turbine
Experimental Setup
CFD
ANSYS
Q-Blade

ABSTRACT

Renewable energies as a clean replacement resource of fossil fuels have many advantages, among which wind has the potential to be the very applicable source in the world. To use wind energy, two kinds of turbines have been developed; the Vertical Axis Wind Turbine (VAWT) and Horizontal Axis Wind Turbine (HAWT). In small scale applications, using a VAWT has some advantages such as low cost and noise, simple mechanism, and the low sensitivity to the wind direction. In this paper, the design and analysis of a combined wind turbine, consist of the Savonius-Darrieus rotor, are performed to use in irrigation applications. To predict the output power, a series of experiments were conducted using the Computational Fluid Dynamics (CFD) method. For this purpose, ANSYS fluent and Q-Blade software programs are used. To design the rotor performance, NACA symmetric airfoils are considered. Next, this combined turbine was made and experimental tests were performed. Finally, the output power is computed and so, the water flow rate for irrigation purposes such as water pumping is obtained. The results indicate that the self-starting of the turbine is improved using the considered design. This could be useful in regions with low wind speed.

1. INTRODUCTION

Nowadays, finding an efficient way to use renewable energies is rapidly growing in all engineering applications. Irrigation, as an example of engineering applications, has been a central feature of agriculture and is the basis of the economy and society of numerous societies. This is the engineering of controlling and harnessing the various natural sources of water, by constructing dams, reservoirs and canals, and finally distributing the water to the agricultural fields, which these operations require a specific amount of energy. This energy can be supplied by either fossil fuels or renewable resources. The limitation of fossil fuels in terms of accessibility and environmental effects resulted in performing renewable energies. Wind as one of the most important renewable energy resources can be used instead of fossil fuels, especially in arid areas with sufficient wind power.

Wind turbines have been used for irrigation and rustic mills since the 7th century AD in the ancient Persia, [1]. So, using wind turbines for irrigation applications such as water pumping operation could be a common purpose for energy consumption. In fact, wind turbine produces the electricity or mechanical energy directly from the kinetic energy of the wind. Wind turbines are classified into two categories: Vertical Axis Wind Turbine (VAWT) and Horizontal Axis Wind Turbine (HAWT). In small scale usage, the VAWT is the most common selection, [2]. In comparison with the HAWT, the VAWT has a simple structure, lower noise, and lower maintenance, [2]. Many studies have been conducted in the case of VAWT design, among which, Eriksson et al. made a comparison between Darrieus and H-Rotor (two most famous VAWT types) wind turbines, [2]. They found that the most advantageous turbine is H-Rotor. El-Samanoudy et al. focused

on the influence of some design parameters of VAWTs; such as the number of blades, pitch angle and the airfoil type, [3]. They realized that using NACA 0021 airfoil, the maximum power coefficient is about 25 % under a 10-degree pitch angle. Castelli et al. converted the basic BEM theory to a CFD code and analyzed a three-bladed wind turbine (NACA 0021 type) performance, [4]. Durrani compared a set of three NACA airfoils (0012, 0015, 0018) and a thicker airfoil size NACA 0022, [5]. He concluded that the NACA 0015 has a more stable performance at the various Tip Speed Ratios (TSRs) than the others. Eleni et al. investigated the behavior of NACA 0012 in various angles of attack. They observed that the k- ω modeling method is the best solving method which was fitted with the experimental data, [6]. Mohammad studied the common symmetrical and unsymmetrical airfoils using the CFD method with the aim of optimizing the power output of the H-rotor turbine, [7]. Sabaefard et al. compared the computational and experimental results of H-rotor VAWT, [8]. They showed that parameters like the airfoil type, blade quantity, and the solidity represent the solving method. Also, the power coefficient was 0.35 in the CFD model and 0.32 in the wind tunnel experiment. Lanzafame et al. studied the comparison between the classical turbulent model and the Shear-Stress Transport (SST) turbulent model, [9]. They obtained a good agreement between the experimental and the CFD results. Joulel et al. compared different NACA airfoil shapes and found that the NACA 00XX airfoil's manufacturing cost is less than the NACA 44XX, [10]. Mohammad et al. focused on the H-rotor performance with different airfoils at low Reynolds numbers, [11]. Two meshing models are compared by using Fluent and Gambit software programs and different solving methods. They achieved that the SST k- ω method is suitable on ANSYS software and the k- ϵ method is realizable on Gambit software. Nguyen et al. investigated the effect of the NACA 00XX thickness on the

*Corresponding Author's Email: p.zarafshan@ut.ac.ir (P. Zarafshan)

starting capability, [12]. They compared four NACA symmetric airfoils and found that the best starting capability is related to the thicker airfoil. Patil et al. considered the CFD analysis of NACA 0012 at different Reynolds numbers and different pitch angles, [13]. These results were compared with the experimental data of Sandia National Laboratory, whereas the lift and the drag coefficient increased in the higher Reynolds number. Sahin and Acir studied the NACA 0015 performance in different Reynolds numbers and different pitch angles, [14]. Extracted results of CFD were compared with the experimental data which were obtained from the wind tunnel test. They found that the best performance of the rotor occurs at the pitch angle of 8° . Hameed and Afaq designed a turbine that its blades shell had a thickness 1 to 5 mm, [15]. They found that decreasing the inner shell thickness from 5 to 2 mm resulted in decreasing distortion and stress.

An experimental study to increase the efficiency of Savonius turbines has been done by [16]. They found the best number of the blade is 2 and the turbine with 2 blades had better power output in all aspect ratios. Also, they found that the combined 2 stage Savonius turbines have more power output. Mohamad Hadi Ali studied the Savonius turbines with 2 and 3 blades, [17]. He found that the coefficient of power for 2 blades was more than 3 blades since an increasing number of blades result in an increasing drag force. The influence of the number of blades on the output power of the Savonius turbine has been investigated by [18]. Turbine with 2, 3 and 4 blades was tested and results showed that the turbine with 3 blades had the best rotation and turbine with 4 blades had the best torque. This result comes from the inverse relation between RPM and torque. Combined Darrieus-Savonius turbine was investigated by [19]. Founded results show better output power for the combined turbine. Also, increasing TSR can result in increasing output power but this increasing limited to a certain point. Gawade et al. compared single Savonius with combined Darrieus-Savonius turbines, [20]. The maximum power coefficient (C_p) is 0.19 and 0.39 for single Savonius and combined turbine, respectively. Akin et al. studied the combined turbine and found that started RPM will be increased in the combined turbine, [21]. Also, the combined turbine could start easily in comparison with a single Darrieus turbine. Chauhan et al. used statistical analysis of wind data with Weibull distribution for analyzing wind probability in Indian State Rajasthan, [22]. The investigation is done at 25 m and 65 m hub height. Most probable speed has been found 5.881 m/s and 6.775 m/s for 25 m and 65 m height correspondingly. Also, the density of mean energy was founded by about 110.006 KWh/m^2 .

In this paper, a combined wind turbine is designed to supply the needed power for water pumping operation. This designed turbine achieved better self-starting performance at low wind speed. To this end, the NACA 0015 symmetrical airfoil has been selected for blades of the H-rotor. Since the low wind speed, Tehran is the pilot of the investigation and so, the wind data were obtained and analyzed. In this regard, the rotor was manufactured with 3 blades and 1.5 m height. Finally, simulation analyses were performed using ANSYS, Fluent and Q-Blade software programs with the wind speed 5.6 m/s.

2. INVESTIGATING METHOD

2.1. Simulation setup

To model the turbine, an H-rotor Darrieus as shown in Fig. 1, has been chosen due to its simple structure. This is the

advantage of H-rotors in comparison with the other Darrieus turbines [2]. For wind speed, collected data, since 2009, were taken from Iran Methodological Organization. Also, Tehran was selected for the investigation pilot. So, data were analyzed with Weibull distribution function, and results showed that the average wind speed is 5.6 m/s. The Weibull and Rayleigh probability density functions are the most common way of analysis of wind speed data and Rayleigh probability density is the special case of Weibull distribution, [23]. To this end, a graphical method has been chosen for the Weibull distribution function. Data of 12 stations within Tehran were studied to achieve the best situation of the wind flow which has enough flow speed during 12 months of the year to perform rotation on the turbine. Most of the studied stations had wind flow less than 3 m/s in the majority of the months. The analysis showed that the best station is located on the northeast part of Tehran (35.7° E , 52.44° N) at Firozkoh Global Atmospheric Watch (GAW). The air properties are summarized in Table 1. After data collection, airfoil type needed to be considered and so, symmetric NACA 00XX airfoils were selected. The most common airfoils among H-rotor turbines, as studied in the literature, are 0012, 0015, 0018 [6]. After airfoil selection, simulations were performed by open source Q-Blade software to ensure the airfoils compatibility (Q-Blade Website). So, all airfoil models (as shown in Fig. 2) were analyzed with Q-Blade software. All simulations were conducted with the chord length 0.18 m and the radius 0.5 m. Double-Multiple Stream-tube Model was used in Q-Blade software for numerical analysis. It should be noted that the mentioned algorithm is applicable for analysis of lift based VAWT. Fig. 3 shows the power coefficient (C_p) for the mentioned three airfoil types, whereas the airfoils NACA 0015 and NACA 0018 show a similar pattern in all TSR values. Also, the best obtained TSR is 3.5. Moreover, the NACA 0012 at TSR 3.5 has the same C_p as the two other models. But, based on the input parameters; height 1.5 m and chord length 0.18 m, it is necessary to consider a stronger rotor which in this study is the thicker one (either NACA 0015 or NACA 0018). Due to the similar behavior of NACA 0015 and NACA 0018 as shown in Fig. 3, and the fact that the thicker airfoil has more weight than the other one, NACA 0015 airfoil was selected as the best case. To validate the obtained results, the performance of NACA 0015 was compared with the existing literature [6-7]. In CFD analysis, ANSYS fluent software was used. The initial data which were obtained from Q-Blade software was set as the input data at ANSYS fluent software. In the next step, a rotor solving domain needs to be defined. For the number of blades in the rotor, the best operational configuration is related to the 3 blades rotor, [4]. Fig. 4 shows the rotor domain with 3 blades that were modeled in ANSYS software. The height and the chord length of blades were selected as 1.5 m and 0.18 m, respectively. To prevent the boundaries' influence on the study, the domain was defined as the square with length $26D$, where D defined as the rotor diameter. The boundary condition was defined for the right and the left borders as the velocity inlet and the pressure outlet, respectively. Also, two symmetrical boundaries were defined in the top and the bottom borders. In the middle of the domain, a circle with 1 m diameter was defined as the rotating zone. Table 2 shows the main characteristics of the designed rotor. All measuring areas meshed with the triangular method. For the area near the blades, the meshing resolution is increased. The meshing structure is shown in Fig. 5. For accurate prediction of the

flow near the blades' wall, the structural mesh with rectangle shape was used as shown in Fig. 6. The maximum value of y^+ for the blades is 60. At first, the simulation was started in fluent software with a steady-state condition. It should be noted that in the simulation, a moving frame was chosen. After 1000 iterations, the simulation was coupled with the other one. In the second simulation, the sliding mesh method was used. Also, the TSR of the rotor was set to be 3.5. So, the angular speed was found to be 40 rad/s. To achieve better quality results, the time step size is 0.00044 sec., which is related to 1 degree rotating of the rotor. Besides, 1800 time steps were selected which is equal to 5 turns of the rotor. For each time step, 50 iterations were also selected, and residuals were adjusted to $1e-5$. After these 1800 time steps, the momentum coefficient, C_m , was captured for one more rotation (360 time steps), concluding the total time step 2160.

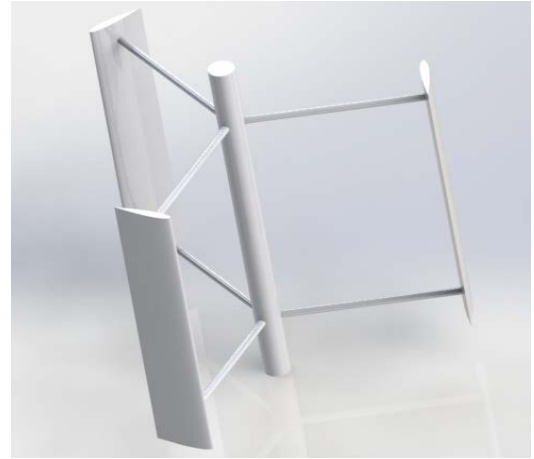


Figure 1. CAD model of H-Rotor turbine.

Table 1. Air standard properties.

Fluid type	Fluid properties		
	Density (kg/m ³)	Viscosity (kg/m-s)	Pressure (Pa)
Air	1.225	1.7894e-05	101325

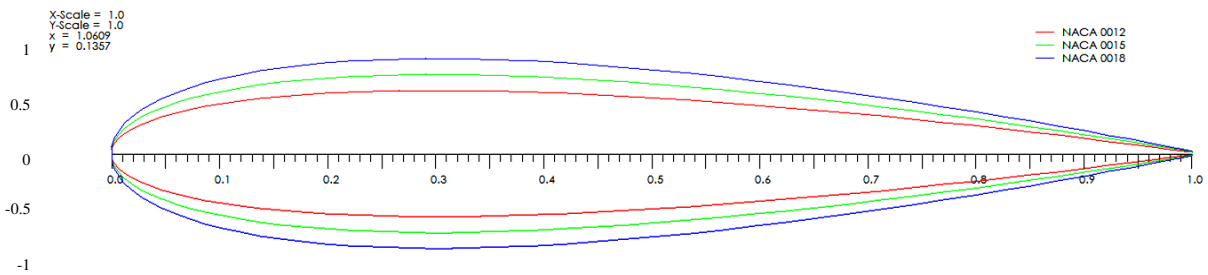


Figure 2. Three blades cross-section.

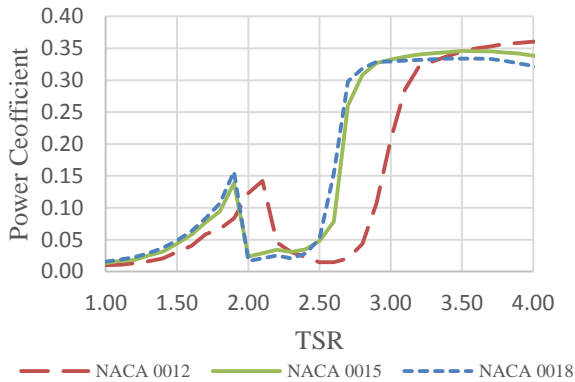


Figure 3. C_p vs TSR simulation result from Q-Blade software.

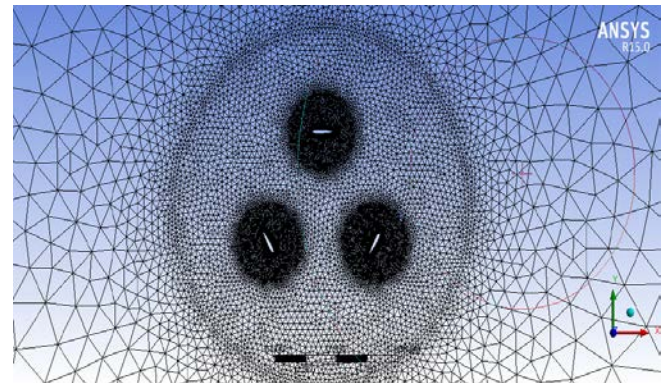


Figure 5. The meshing structure.

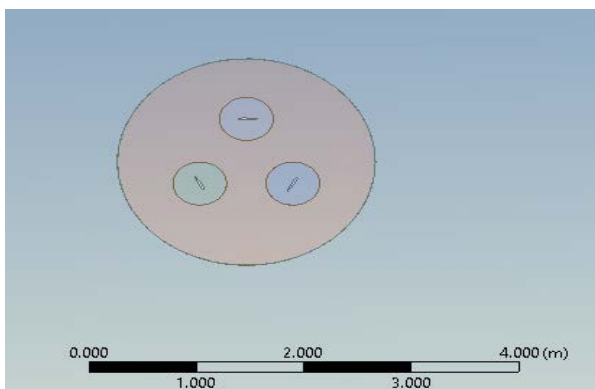


Figure 4. Model of the domain in ANSYS software.

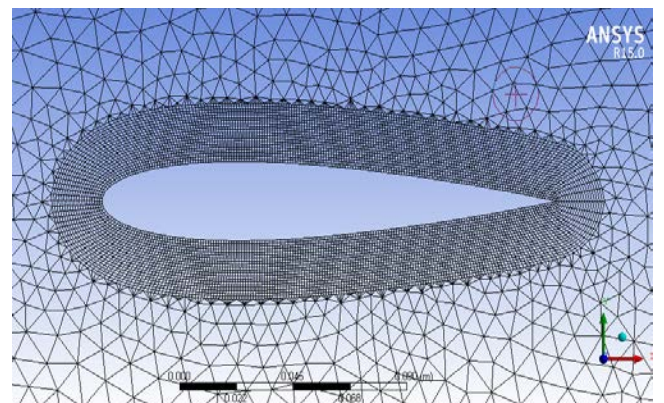


Figure 6. Structure of the mesh near the blades.

In addition, the realizable $k - \epsilon$ solving method was selected. For the solution method, the pressure-velocity coupled was chosen. Prismo solving method was selected for the pressure and momentum. Also, the turbulent kinetic energy and turbulent dissipation rate were adjusted to the second-order upwind. So, the accuracy and the total solving time of simulation were increased. This method is the most popular for the prediction of rotating turbines, [12]. Also, the

realizable $k - \epsilon$ solving method can predict the flow near the blades in the strong pressure gradient areas better than the standard $k - \epsilon$ method, [12]. Besides, for the Savonius turbine, simulations are done in ANSYS software, which has 50 cm diameter and 40 cm height (Fig. 7). The steady situation was selected for time and also, 2000 iterations were performed.

Table 2. Design features of simulated rotor.

Denomination	Features				
	Height	Diameter	No. of blades	Chord length	Blade section
Rotor	1.5 m	1 m	3	0.18 m	NACA0015

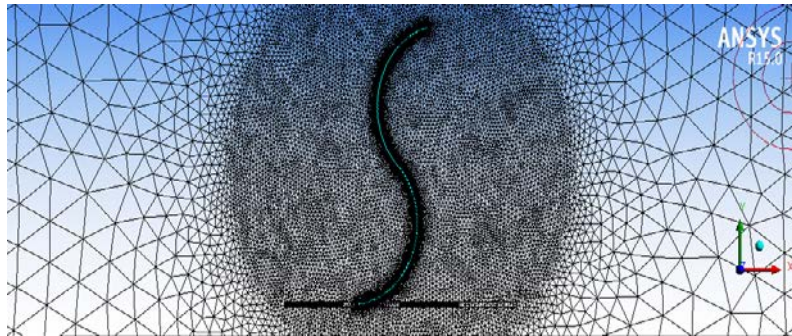


Figure 7. Meshing of Savonius turbine in ANSYS Software.

2.2. Mathematical equations

Weibull distribution equation can be stated as:

$$F(v) = \left(\frac{k}{C}\right) \cdot \left(\frac{v}{C}\right)^{k-1} \cdot \exp\left[-\left(\frac{v}{C}\right)^k\right] \quad (1)$$

where C and k are defined as the Weibull scale and shape parameters, respectively. For the graphical method, Eq. (1) is converted to the logarithmic form as:

$$\ln[-\ln(1 - F(v))] = k \times \ln(v) - k \times \ln(C) \quad (2)$$

By plotting $\ln(v)$ and $[-\ln(1 - F(v))]$, the Weibull scale and shape parameters are achievable, [24]. To find the power coefficient of rotor, Fluent software could give C_m . Total available power which could achieve from the wind is related to the wind speed (v_∞), the total area of passing flow from the rotor (A) and the flow density (ρ) as:

$$P_{max} = \frac{1}{2} \rho V_\infty^3 A \quad (3)$$

Power coefficient is described as the power ratio which the rotor could gain from the flow to the total available power as:

$$C_p = \frac{P}{P_{max}} \quad (4)$$

Also, the non-dimensional lift, drag and moment coefficient are, [25]:

$$C_L = \frac{L}{q_\infty S}, C_D = \frac{D}{q_\infty S}, C_M = \frac{M}{q_\infty S l} \quad (5)$$

where L is the lift force, S is the reference area, q_∞ is the dynamic pressure of the flow, D and M are the drag force and

pitching moment, respectively, and l is the reference length. The TSR ratio is also defined as:

$$\lambda = \frac{r\omega}{V_\infty} \quad (6)$$

where r is the rotor radius and ω is the angular velocity. Total C_p is given by C_m as, [26]:

$$C_p = C_m \lambda \quad (7)$$

2.2.1. Realizable $k - \epsilon$ solving method

Reynolds-averaged Navier-Stokes equation can be given as:

$$\frac{\partial}{\partial t}(\rho u_i) + \frac{\partial}{\partial x_j}(\rho u_i u_j) = -\frac{\partial p}{\partial x_i} + \frac{\partial}{\partial x_i} \left[\mu \left(\frac{\partial u_i}{\partial x_j} + \frac{\partial u_j}{\partial x_i} - \frac{2}{3} \delta_{ij} \frac{\partial u_k}{\partial x_k} \right) \right] + \frac{\partial}{\partial x_j}(-\rho \overline{u'_i u'_j}) \quad (8)$$

The non-linear term of equation or $(-\rho \overline{u'_i u'_j})$ described the fluctuation still appear in RANS. This influence is called the Closure problem. To solve this problem, Boussinesq introduced the concept of eddy viscosity. This theory shows that the transfer momentum is caused by turbulence. It could be modeled with the eddy viscosity. The relationship between the Reynold stress tensor and the strain tensor can be defined as:

$$\tau_{ij} = 2\mu_t S_{ij} - \frac{2}{3} \rho k \delta_{ij} \quad (9)$$

where μ_t or the eddy viscosity is a scalar property and so:

$$-\rho \overline{u'_i u'_j} = \mu_t \left(\frac{\partial u_i}{\partial x_j} + \frac{\partial u_j}{\partial x_i} \right) - \frac{2}{3} (\rho k + \mu_t \frac{\partial u_k}{\partial x_k}) \delta_{ij} \quad (10)$$

Being of Reynolds stress tensor as the proportion of the strain tensor is the main disadvantage of Boussinesq theory.

Future model like the $k-\varepsilon$ developed model covers this shortcoming. The transport equations can be given as:

$$\frac{\partial}{\partial t}(\rho k) + \frac{\partial}{\partial x_j}(\rho k u_j) = \frac{\partial}{\partial x_j} \left[\left(\mu + \frac{\mu_t}{\sigma_k} \right) \frac{\partial k}{\partial x_j} \right] + p_k + p_b \quad (11)$$

$$+ \rho \varepsilon - Y_M + S_k$$

and:

$$\frac{\partial}{\partial t}(\rho \varepsilon) + \frac{\partial}{\partial x_j}(\rho \varepsilon u_j) = \frac{\partial}{\partial x_j} \left[\left(\mu + \frac{\mu_t}{\sigma_\varepsilon} \right) \frac{\partial \varepsilon}{\partial x_j} \right] + \rho C_1 S_\varepsilon \quad (12)$$

$$- \rho C_2 \frac{\varepsilon^2}{k + \sqrt{v\varepsilon}} + C_{1\varepsilon} \frac{\varepsilon}{k} C_{3\varepsilon} P_b + S_\varepsilon$$

where:

$$S = \sqrt{2S_{ij}S_{ij}}, C_1 = \max\left[0.43, \frac{\eta}{\eta+5}\right], \eta = S \frac{k}{\varepsilon} \quad (13)$$

and the model constants are:

$$C_{1\varepsilon} = 1.44, C_2 = 1.9, \sigma_k = 1.0, \sigma_\varepsilon = 1.2 \quad (14)$$

It is important to note that this model is known as the most expensive computationally model, [27].

2.3. Experimental setup

Turbines were modeled in Solidworks software as shown in Fig. 8. Each blade of the Darrieus turbine is divided into a few smaller sections. As shown in Fig. 9, balsa wood has been chosen as a blades material with the aim of low weight and good shapeable capability. Then, laser cutting CNC machine has been used to achieve good accuracy of shape sections. Also, this figure shows Balsa wood with a thickness of 1.5 mm which is used for covering sections. To improve the stability of the structure, a balsa pole with a square cross-section was selected and all sections were mounted with a distance of 10 cm. Moreover, aluminum was chosen for the main turbine shaft. For mounting blades on the mentioned shaft, 9 tubes of fiber glass with a diameter of 7.5 mm were chosen. Epoxy glue was selected for the tightening of the fiber glass tube to balsa wood blades and the main aluminum shaft. For the Savonius turbine, sheet metal with a thickness of 1 mm was used. Also, 2 circles with diameter 50 cm were mounted to the curve blades by spot welding to keep the blades. To prevent vibration, the main shaft was tightened from 3 points with the bearing system. 2 iron plates with the weight of 35 Kg were used for keeping turbine stability during its rotations. To run the experimental condition, a blower with 4 axial fans was used for the turbine test. For adjusting fans' speed, a dimmer was placed between the fans and the power source. For measurement of the wind speed, an anemometer was used. Static torque was measured by a digital torque meter. To study the influence of the Savonius turbine, the coupling system was added between two turbines. Finally, the designed experimental setup is shown in Fig. 10.

3. RESULTS AND DISCUSSION

Weibull distributions of 12 stations were investigated and it found that the best station with the most probability of wind flow at year is Firozko GAW. The scale and shape coefficient of Weibull distribution is 6.25 and 1.513, respectively. This Weibull distribution with the graphical method is shown in Fig. 11. The average wind speed finds as

5.6 m/s and the maximum speed is 10 m/s. So, TSR is considered as 3.5 for the selected NACA 0015 blades which are used for the simulation to achieve the best prediction of C_p . The output average value of C_m from ANSYS and Fluent software programs is 0.04. To find the C_p coefficient, Eq. 7 has been used and it is calculated as 0.14. To approve the obtained value, a simulation was done in Q-Blade software. Q-Blade software predicts the value of C_p in TSR 3.5 for the NACA 0015 about 0.34 as shown in Fig. 12. Also, the total achievable energy from the wind is calculated as 164.4 Wh. According to the Betz limit, the maximum value of C_p is 0.59. Thus, the total available power from the wind is 97 Wh. With the obtained data from the simulation, the considered H-rotor can produce 52.8 Wh. According to the torque coefficient which is found from simulation and using Eq. 5, the total achievable torque is 0.58 N.cm. After separating two turbines, experimentally maximum static torque for Darrieus wind turbine is found 0.48 N.cm. Then, both turbines are coupled and the blower speed adjusted with dimmer. As shown in Fig. 13, torque coefficient was measured at different wind speed and results were compared with simulation. In the low wind speed, simulation results were less than experimental results because of the low accuracy of the simulation in low Reynolds numbers. Also, with increasing the wind speed because of the existence of the Savonius turbine in an actual situation, experimental results show lower values than the simulation. The main reason for this leakage is the fact that the Savonius turbine's behavior changed during increasing the wind speed and after increasing the wind speed this kind of turbine produced negative torque. It found that after the wind speed reaches 4 m/s, the Savonius turbine easily could start to rotate both turbines. In the simulation of the Savonius turbine, it was found that with the wind speed 3 m/s, the produced turbine torque would be enough to start the rotation according to the low weight of Darrieus turbine (Fig. 14). The output power of the turbine can be used to produce a static head on the water level for irrigation purposes. To this end, it founds that with the simulation output values, the water can be pumped to 10 m height with the flow rate 1.9 m³/h. Also, the obtained experimental results show the flow rate 0.84 m³/h. The difference between these two values related to the simulation and the actual conditions is the fact that Savonius turbine's behavior changed during increasing the wind speed and after increasing the wind speed this kind of turbine produced negative torque.

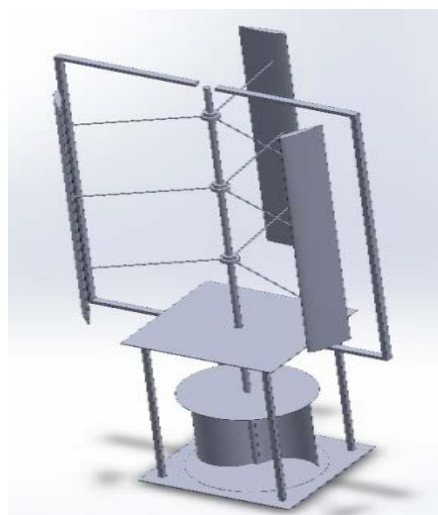


Figure 8. Modeled combined wind turbine.



Figure 9. Covered sections with Balsa wood.



Figure 10. Desigend experimental setup.

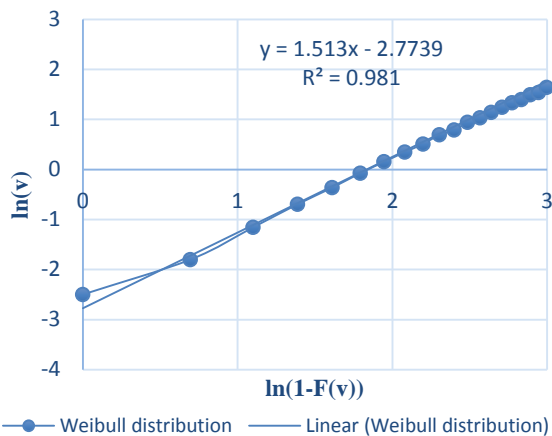


Figure 11. $\ln(v)$ vs $\ln(1-F(v))$ scheme for scale and shape parameter of Weibull distribution.

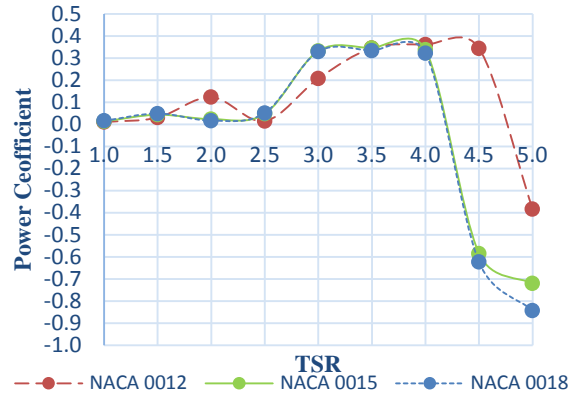


Figure 12. C_p vs TSR from Q-Blade software for 3 NACA symmetric airfoils.

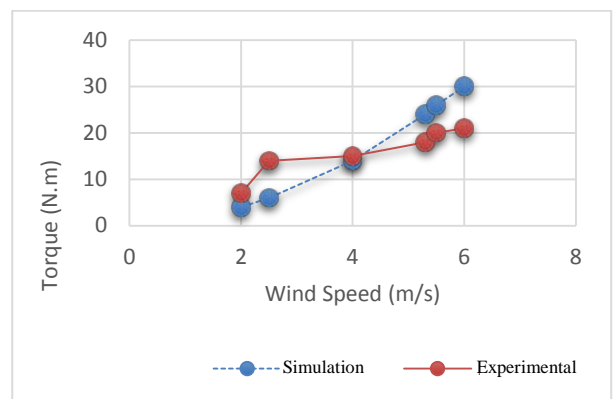


Figure 13. Comparison between produced torque in the experiment and the simulation.

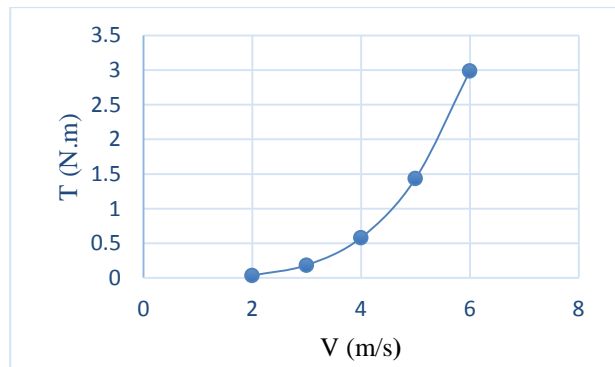


Figure 14. Produced torque in the simulation of Savonius turbine in ANSYS software.

4. CONCLUSIONS

In this paper, the design and analysis of an H-rotor wind turbine with the purpose of irrigation applications were considered. In which, Tehran was chosen as the pilot of the investigation since its low-speed wind. This wind speed required the designed combined wind turbine. Next, the simulation was performed. According to the results, the best station with the most probability of wind along one year was Firozkoh. The maximum and the mean wind speed value of this pilot were 10 m/s and 5.6 m/s, respectively. Also, the best performance of blades for the H-rotor turbine was related to the NACA 0015. As expected, the best value of TSR for NACA 0015 was considered as 3.5. Finally, the output power was computed and so, the water flow rate for irrigation

purposes such as water pumping was obtained. The results indicated that the self-starting of the turbine was improved using the considered design.

5. ACKNOWLEDGEMENT

The authors would like to thank the financial support provided by University of Tehran for accomplishing this research.

REFERENCES

- Prasad, S. and Auradi, V., "Optimized design of rotor blade for a wind pump", *International Journal of Renewable Energy Research (IJRER)*, Vol. 2, No. 4, (2012), 746-749.
- Eriksson, S., Bernhoff, H. and Leijon, M., "Evaluation of different turbine concepts for wind power", *Renewable and Sustainable Energy Reviews*, Vol. 12, No. 5, (2008), 1419-1434. (<https://doi.org/10.1016/j.rser.2006.05.017>).
- El-Samanoudy, M., Ghorab, A. and Youssef, S.Z., "Effect of some design parameters on the performance of a Giromill vertical axis wind turbine", *Ain Shams Engineering Journal*, Vol. 1, No. 1, (2010), 85-95. (<https://doi.org/10.1016/j.asej.2010.09.012>).
- Castelli, M.R., Englaro, A. and Benini, E., "The Darrieus wind turbine: Proposal for a new performance prediction model based on CFD", *Energy*, Vol. 36, No. 8, (2011), 4919-4934. (<https://doi.org/10.1016/j.energy.2011.05.036>).
- Durrani, N., "A detailed aerodynamic design and analysis of a 2D vertical axis wind turbine using sliding mesh in CFD", *Proceedings of 49th AIAA Aerospace Sciences Meeting and Exhibition*, (2011).
- Eleni, D.C., Athanasios, T.I. and Dionissios, M.P., "Evaluation of the turbulence models for the simulation of the flow over a National Advisory Committee for Aeronautics (NACA) 0012 airfoil", *Journal of Mechanical Engineering Research*, Vol. 4, No. 3, (2012), 100-111. (<https://doi.org/10.5897/JMER11.074>).
- Mohamed, M., "Performance investigation of H-rotor Darrieus turbine with new airfoil shapes", *Energy*, Vol. 47, No. 1, (2012), 522-530. (<https://doi.org/10.1016/j.energy.2012.08.044>).
- Sabaefard, P., Razzaghi, H. and Forouzandeh, A., "Determination of vertical axis wind turbines optimal configuration through CFD simulations", *Proceedings of International Conference on Future Environment and Energy*, (2012).
- Lanzafame, R., Mauro, S. and Messina, M., "2D CFD modeling of H-Darrieus wind turbines using a transition turbulence model", *Energy Procedia*, Vol. 45, (2014), 131-140. (<https://doi.org/10.1016/j.egypro.2014.01.015>).
- Jouilel, N., Radouani, M. and El Fahime, B., "Geometric modeling and contribution to the choice of a blade profile", *Proceedings of Xème Conférence Internationale: Conception et Production Intégrées*, (2015).
- Mohamed, M., Ali, A. and Hafiz, A., "CFD analysis for H-rotor Darrieus turbine as a low speed wind energy converter", *Engineering Science and Technology, an International Journal*, Vol. 18, No. 1, (2015), 1-13. (<https://doi.org/10.1016/j.jestch.2014.08.002>).
- Nguyen, C., Le, T. and Tran, P., "A numerical study of thickness effect of the symmetric NACA 4-digit airfoils on self starting capability of a 1KW H-type vertical axis wind turbine", *International Journal of Mechanical Engineering and Applications (IJMEA)*, Vol. 3, No. 3-1, (2015), 7-16. (<https://doi.org/10.11648/j.ijmea.s.2015030301.12>).
- Patil, B.S. and Thakare, H.R., "Computational fluid dynamics analysis of wind turbine blade at various angles of attack and different Reynolds number", *Procedia Engineering*, Vol. 127, (2015), 1363-1369. (<https://doi.org/10.1016/j.proeng.2015.11.495>).
- Şahin, İ. and Acir, A., "Numerical and experimental investigations of lift and drag performances of NACA 0015 wind turbine airfoil", *International Journal of Materials, Mechanics and Manufacturing*, Vol. 3, No. 1, (2015), 22-25. (<https://doi.org/10.7763/IJMMM.2015.V3.159>).
- Hameed, M.S. and Afaq, S.K., "Design and analysis of a straight bladed vertical axis wind turbine blade using analytical and numerical techniques", *Ocean Engineering*, Vol. 57, (2013), 255-248. (<https://doi.org/10.1016/j.oceaneng.2012.09.007>).
- Mahmoud, N.H., El-Haroun, A.A., Wahba, E. and Nasef, M.H., "An experimental study on improvement of Savonius rotor performance", *Alexandria Engineering Journal*, Vol. 51, No. 1, (2012), 19-25. (<https://doi.org/10.1016/j.aej.2012.07.003>).
- Ali, M.H., "Experimental comparison study for Savonius wind turbine of two & three blades at low wind speed", *International Journal of Modern Engineering Research (IJMER)*, Vol. 3, No. 5, (2013), 2978-2986.
- Wenehenubun, F., Saputra, A. and Sutanto, H., "An experimental study on the performance of Savonius wind turbines related with the number of blades", *Energy Procedia*, Vol. 68, (2015), 297-304. (<https://doi.org/10.1016/j.egypro.2015.03.259>).
- Sharma, K.K., Biswas, A. and Gupta, R., "Performance measurement of a three-bladed combined Darrieus-Savonius rotor", *International Journal of Renewable Energy Research*, Vol. 3, No. 4, (2013), 885-891.
- Gawade, S.G. and Patil, D.S., "Comparative study of a single stage Savonius with a combined Savonius-three bladed Darrieus", *International Journal For Technological Research In Engineering (IJTRE)*, Vol. 2, No. 6, (2015), 542-545.
- Ilhan, A., Bilgili, M. and Sahin, B., "Analysis of aerodynamic characteristics of 2 MW horizontal axis large wind turbine", *Wind and Structures, An International Journal*, Vol. 27, No. 3, (2018), 187-197. (<https://doi.org/10.12989/was.2018.26.3.187>).
- Chauhan, A. and Saini, R.P., "Statistical analysis of wind speed data using Weibull distribution parameters", *Proceedings of IEEE 1st International Conference on Non Conventional Energy (ICONCE)*, Kalyani, India, (2014). (<https://doi.org/10.1109/ICONCE.2014.6808712>).
- Celik, A.N., "Assessing the suitability of wind energy speed probability distribution functions based on wind power density", *Renewable Energy*, Vol. 28, (2003), 1563-1574.
- Kidmo, D., "Statistical analysis of wind speed distribution based on six Weibull methods for wind power evaluation in Garoua, Cameroon", *Revue des Energies Renouvelables*, Vol. 18, No. 1, (2015), 105-125.
- Anderson Jr, J.D., *Fundamentals of aerodynamics*, Tata McGraw-Hill Education, (2010).
- Patel, M.B. and Kevat, V., "Performance prediction of straight bladed Darrieus wind turbine by single streamtube model", *International Journal of Advanced Engineering Technology (IJAET)*, Vol. 14, No. 2, (2013), 86-89.
- Marzouk, O.A. and Huckaby, E.D., "Simulation of a swirling gas-particle flow using different k-epsilon models and particle-parcel relationships", *Engineering Letters*, Vol. 18, No. 1, (2010).